FINE-GRAINED, SPINEL-RICH Ca-Al-RICH INCLUSIONS FROM THE REDUCED CV3 CHONDRITE EFREMOVKA: A GENETIC LINK TO WARK-LOVERING RIMS? J. Han[1,2] and L. P. Keller[2], [1]Lunar and Planetary Institute, USRA, 3600 Bay Area Boulevard, Houston, TX 77058, USA (jangmi.han@nasa.gov), [2]ARES, Code XI3, NASA Johnson Space Center, 2101 NASA Parkway, Houston, TX 77058, USA.

Introduction: Fine-grained, spinel-rich Ca-Al-rich inclusions (FGIs) in carbonaceous chondrites, mostly CV3 chondrites, are interpreted as aggregates of nebular gas-solid condensates that escaped significant melting [1]. Multiple lines of evidence suggest a condensation origin for FGIs, including their layered structures and irregular shapes and the fine grain size of numerous spinel-cored nodules [e.g., 2,3], and the distinctive volatility-fractionated group II rare earth element patterns of bulk inclusions and their mineral constituents [e.g., 4,5]. The origin and nature of FGIs are poorly constrained because of their fine grain sizes and intimate intergrowths of refractory phases, combined with their susceptibility to secondary parent body alteration processes, making detailed mineralogical and petrologic characterizations difficult using scanning electron microscope (SEM) and electron microprobe techniques.

In this study, we present preliminary transmission electron microscope (TEM) analyses of pristine FGIs from the reduced CV3 chondrite Efremovka in order to provide the detailed characterization of their micrometer- to nanometer-scale textures and chemical compositions. Our goals are to better understand the formation processes and conditions of FGIs in the early solar nebula and to explore their possible genetic relationship with other early-formed refractory inclusions and their rims.

Methods: In our initial survey of FGIs from the reduced CV3 chondrites, we identified 6 FGIs from two thin sections of Efremovka. We used a FEI Quanta 3D field emission gun SEM/focused ion beam (FIB) instrument in order to document the detailed petrologic and mineralogical characteristics of these FGIs and to prepare two TEM sections from FGI *A-01*. The sections were examined in detail using a JEOL 2500SE field emission scanning TEM equipped with a Thermo-Noran thin window energy dispersive X-ray (EDX) spectrometer.

Results: The Efremovka FGIs are irregularly shaped inclusions (up to ~4 mm in size) that have a common internal structure consisting of numerous nodules of spinel ± hibonite ± perovskite, each nodule is surrounded by monomineralic layers of ±melilite, ±anorthite, and pyroxene (**Fig. 1**). The FGIs do not show a concentric mineral zoning with a distinct core-mantle structure, as described by [3], instead show a uniform texture and mineralogy throughout. Significant variations in modal abundance and grain size of constituent minerals among the inclusions are observed. None of the FGIs are porous or surrounded by olivine-rich accretionary rims. The majority of Efremovka FGIs show little evidence for secondary parent body alteration from Na- and Fe-rich fluids. One exception is FGI *A-03* containing melilite and anorthite that had been extensively replaced by nepheline, similar to FGIs from the oxidized CV3 chondrite Allende [e.g., 6,7].

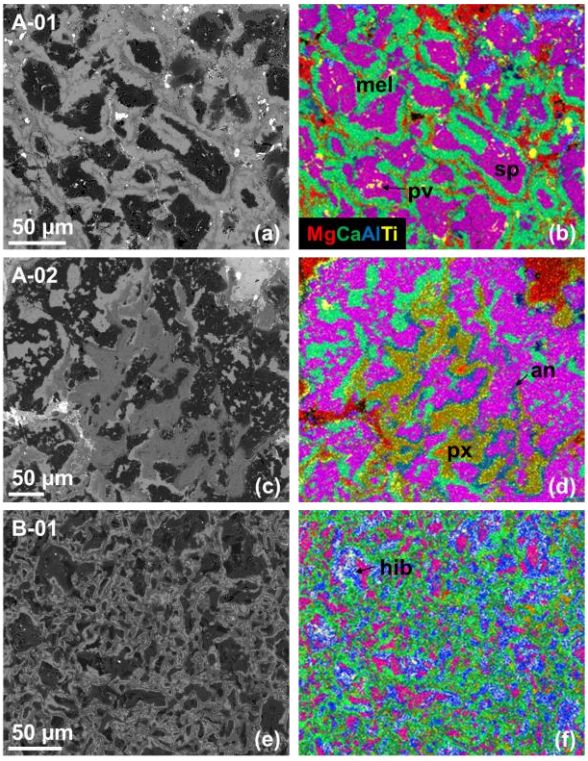

Figure 1. (a,c,e) BSE images and (b,d,f) corresponding false color X-ray maps (Mg=red, Ca=green, Al=blue, Ti=yellow) of Efremovka FGIs.

FGI *A-01* has the typical structure of irregularly shaped nodules of spinel with minor hibonite and perovskite that are surrounded successively by melilite, ±anorthite, diopside, and olivine (**Fig. 1a,b**). Our TEM analyses of two FIB sections from FGI *A-01* showed that thin, discontinuous layers (≤1 µm) of Al-Ti-rich pyroxene are present, separating spinel from melilite and that melilite contains fine inclusions of spinel just below anorthite (**Fig. 2**). Pods of fine-grained, Mg-rich materials (likely Mg-rich olivine + other minor phases) occur between the nodules. Individual mineral phases in the inclusion share the following microstructural

features: (1) each consists of compact aggregates of micrometer to sub-micrometer sized crystals; (2) highly curved grain boundaries between minerals are frequently observed; (3) crystallographic orientation relationships between adjacent minerals are uncommon, with most grains showing random orientations towards each another; and (4) most minerals are defect free, except for hibonite that has abundant stacking faults. High dislocation densities and considerable strain are common in melilite and spinel, indicative of shock deformation. In addition, our TEM EDX analyses revealed oscillatory Ti zoning in hibonite (~4-7 wt% TiO_2) as well as systematic decreases in Al_2O_3 contents in melilite and in Al_2O_3 and TiO_2 contents in pyroxene moving outwards. Spinel contains up to ~20 wt% FeO, but typically ≤5 wt%, whereas melilite and anorthite do not show Na concentration.

Discussion: Collectively, the observed layered structure and fine-grained nature of the Efremovka FGIs and the decrease in volatility through mineral layers in their individual nodules confirm that the inclusions formed by condensation. The fine scale layering preserved in the individual nodules may reflect evolving condensation and gas-solid reactions, but the reactions clearly did not go to completion, protecting underlying grains from further back reactions [8]. The inferred mineral formation sequence from the FGIs differs from the predictions of thermodynamic models [9], indicating that they formed under non-equilibrium conditions.

We infer sequential events of condensation and gas-solid reactions to form FGI *A-01* that occurred in the early solar nebula, as follows. (1) Hibonite and perovskite appear to be the first phases to condense. (2) The occurrence of stacking faults in hibonite may represent complex intergrowths of stoichiometric and disordered, Mg-enriched hibonite as a result of the structural modification by forming wider spinel blocks [10]. This suggests that hibonite incompletely reacted with gaseous Mg and was partially replaced by spinel. (3) Al-Ti-rich pyroxene formed after spinel, but a reaction with spinel requires Ti in the gas phase [11]. (4) Melilite and diopside formed through a reaction with gaseous Mg and SiO, as predicted by [9]. (5) Anorthite is minor and discontinuous, but its highly embayed and scalloped interfaces with underlying melilite are apparent, suggesting that melilite was replaced by anorthite after pyroxene formation [3]. (6) Minor forsterite condensed as the final formation stage. TEM analyses of the pods of fine grained, Mg-rich materials between the nodules are underway to determine if these materials represent high-temperature condensates aggregated in the early solar nebula or matrix materials that were accreted on the parent body.

Based on their bulk compositions and mineral assemblages, FGIs were inferred as probable precursors of condensation assemblages for type C inclusions [e.g., 3]. In fact, the textural and mineralogical features of FGIs described above are remarkably similar to those observed from Wark-Lovering (WL) rims [12], suggesting the possibility of a genetic relationship between these two. Further coordinated analyses, including isotopic measurements, should better elucidate these relationships.

Conclusions: We conducted a very first TEM analysis of a pristine FGI *A-01* from the reduced CV3 chondrite Efremovka, which characterizes its primary structure and mineral assemblages. This allows us to explore the details of condensation and gas-solid reactions in the early solar nebula and a possible genetic relationship between FGIs and WL rims.

Acknowledgements: This study was supported by NASA grant 17-EW17_2-0148 to LPK. Dr. Zolensky is thanked for allocation of the CV3 chondrite Efremovka.

References: [1] MacPherson G. J. (2014) In Treatise on Geochemistry II, vol.1, pp.139-179. [2] Holmberg B. B. & Hashimoto A. (1992) Meteoritics 27, 149-153. [3] Krot A. N. et al. (2004) MAPS 39, 1517-1553. [4] Tanaka T. & Masuda A. (1973) Icarus 19, 523-530. [5] Huss G. R. et al. (2002) MAPS 37, A68. [6] Kornacki A. S. & Wood J. A. (1985) GCA 49, 1219-1237. [7] McGuire A. V. & Hashimoto A. (1989) GCA 53,1123-1133. [8] Petaev M. I. & Wood J. A. (2005) In Chondrites and Protoplanetary Disk, vol.341, pp.373-406. [9] Yoneda S. & Grossman L. (1995) GCA 59, 3413-3444. [10] Han J. et al. (2015) MAPS 50, 2121-2136. [11] Han J. & Brearley A. J. (2017) GCA 201, 136-154. [12] Han J. et al. (2015) 78th MetSoc, abstract #5243.

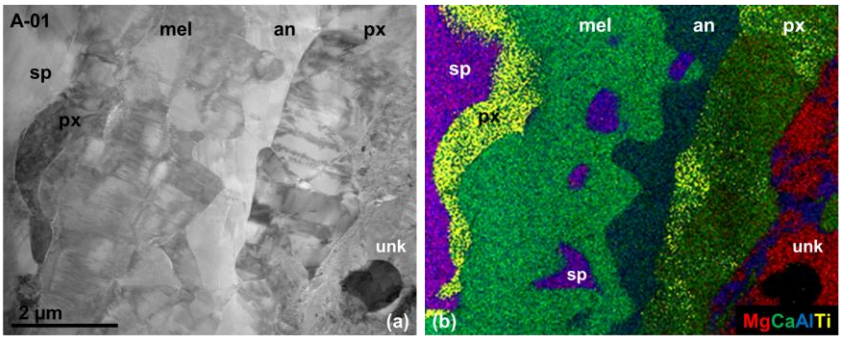

Figure 2. (a) BF STEM image and (b) corresponding false color X-ray map (Mg=red, Ca=green, Al=blue, Ti=yellow) of FGI *A-01*.